



Original Article

Enhancement of Magnetic Field Strength and Gradient Produced by an Array of Micro-sized Parallelepiped Magnets

Nguyen Huy Tiep, Bui Dinh Tu, Le Viet Cuong*

VNU University of Engineering and Technology, 144 Xuan Thuy, Cau Giay Hanoi, Vietnam

Received 20 August 2022

Revised 05 October 2022; Accepted 10 October 2022

Abstract: In this work, we carried out survey on magnetic field strength and gradient in space around arrays of micro-sized parallelepipedic magnets by simulation and calculation. Magnetic field distributions are a function of magnet's size and position with respect to magnet's surface. Our purpose is to explain how magnetic interactions evolve while dimensions of magnetic sources are reduced. Firstly, the simulations and calculations were executed for a magnet with a large surface size of $1,000 \times 1,000 \mu\text{m}^2$, a thickness of $5 \mu\text{m}$, and a residual magnetism of 1.6T perpendicular to its surface. Then, the similar works were also performed for arrays of magnets with smaller surface sizes, e.g. $1,000 \times 500 \mu\text{m}^2$; $1,000 \times 200 \mu\text{m}^2$; $1,000 \times 100 \mu\text{m}^2$; $1,000 \times 50 \mu\text{m}^2$ and $1,000 \times 10 \mu\text{m}^2$. Consequently, both the magnetic field strength and gradient in the space which is above and near the surface of the magnets, particularly, the space from the surface of the magnets to the height of $100 \mu\text{m}$ far from the surface of the magnets, were enhanced when the magnets' size were appropriately reduced. This suggests that the application field of the magnets will be expanded and their integration into microsystems will be grown as the size of the magnets is reduced.

Keywords: Magnets, micro magnets, magnetic field strength, magnetic field gradient.

1. Introduction

As we know, permanent magnets (often just called magnets) have been used in many different areas and for many various functions in a few past decades. Common applications of magnets can be listed as loudspeakers, meters, watches, weighing systems, microwave ovens, motors, cameras, typewriters,

* Corresponding author.

E-mail address: cuonglv@vnu.edu.vn

<https://doi.org/10.25073/2588-1124/vnumap.4770>

voice and video recorders, and so on. Nowadays, magnets have an important role in communication devices such as telephones, computers, laptops; in particle accelerators; also, in nuclear magnetic resonance imagers for medical applications. They are also employed in suspension and impulsion units for magnetically levitated vehicles [1]. One of the newest applications of magnets is like traps to separate, control, attract, and push micro-objects such as magnetic beads, and biological molecules [2-4]. Since these micro-objects are very small in size and mass, to exert a magnetic force on them requires the magnets to have a large magnetic field strength and gradient, along with a relatively small size. Thus, many magnetic aspects such as the kind of magnets, their strength, their size, their number, their shape, and configuration are needed to consider when designing parameters for magnets and calculating magnetic quantities. Some papers studying the geometry [4-6], the magnetic anisotropy [7], and the materials [3] for magnets have been reported so far. Whereas, the authors of [4, 8] have discussed on the magnets at either micro- or large scales. However, to the best of our knowledge, few systemic studies on the variation of the spatial distribution of magnetic field produced by magnets when changing the size and the configuration of magnets have been so far reported. So, this work, by simulation and calculation, is focused on the enhancement of the magnetic field produced by parallelepiped magnets according to different sizes and configurations. We studied magnets with the following parameters: the residual magnetism ($\mu_0 M$) of 1.6T along the z axis (this value is suitable for thin films of Nd₂Fe₁₄B [9, 10]), i.e. perpendicular to the surface of magnets, the thickness of 5 μm , the surface area of magnets decreasing from 1,000 \times 500 μm^2 to 1,000 \times 10 μm^2 while the number of magnets increasing from 1 magnet to 50 magnets, the distance between magnets of 10 μm .

2. Calculations and Simulations

In this work, we applied the calculation and simulation models of Camacho et al., [5], Bancel et al., [11], and Yang et al., [12] based on the Coulombian approach and the superposition principle to calculate components of the magnetic induction of the magnets. Let's consider a magnet shown in Fig. 1. Its dimensions are 2a, 2b, and 2c along the x, y, and z axis, respectively. Its magnetization is denoted by \vec{M} on the z axis. To calculate the induction field at point $\vec{r} = (x; y; z)$ produced by the magnet, we divide the magnet into infinitesimal magnetic dipoles. Each dipole has a volume of $dV = dx'dy'dz'$, a magnetic moment of $d\vec{m} = \vec{M}dV$, and induces a magnetic scalar potential of $d\phi$ at the point \vec{r} .

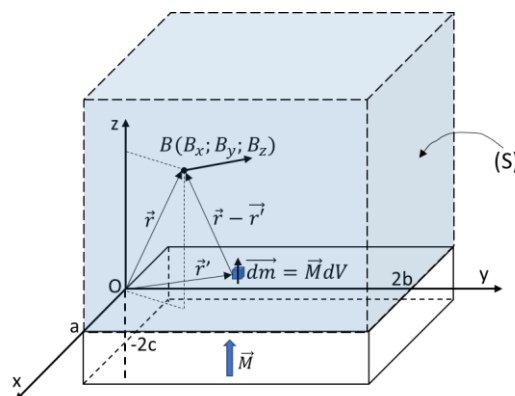


Figure 1. Scheme for calculating the magnetic field induction produced by a parallelepiped magnet.

The potential (expressed in Ampere) at the point \vec{r} produced by the dipole at point $\vec{r}' = (x'; y'; z')$ is given by:

$$\begin{aligned} d\phi &= \frac{1}{4\pi} \frac{\vec{dm} \cdot (\vec{r} - \vec{r}')}{|\vec{r} - \vec{r}'|^3} = \frac{1}{4\pi} \frac{dm \cdot \cos(\vec{dm}, (\vec{r} - \vec{r}'))}{|\vec{r} - \vec{r}'|^2} = \frac{1}{4\pi} \frac{MdV(z - z')}{|\vec{r} - \vec{r}'|^3} \\ &= \frac{M}{4\pi} \frac{z - z'}{[(x - x')^2 + (y - y')^2 + (z - z')^2]^{3/2}} dx' dy' dz' \end{aligned}$$

The total scalar potential at the point \vec{r} is then given by:

$$\phi = \int_V d\phi = \frac{M}{4\pi} \int_{-a}^a \frac{dx'}{[(x - x')^2 + (y - y')^2 + (z - z')^2]^{3/2}} \int_0^{2b} dy' \int_{-2c}^0 (z - z') dz'$$

Then, magnetic field (expressed in Tesla) is taken by: $\vec{B} = -\mu_0 \nabla \phi$

Finally, we get expressions for the B_x, B_y, B_z components of the magnetic induction vector \vec{B} at any point as the below:

$$B_x = \frac{\mu_0 M}{4\pi} \ln \left[\frac{F_1 F_2}{F_3 F_4} \right]$$

with:

$$F_1 = \frac{\sqrt{(-x + a)^2 + (y - 2b)^2 + (-z + 2c)^2} + 2b - y}{\sqrt{(-x + a)^2 + y^2 + (-z + 2c)^2} - y}$$

$$F_2 = \frac{\sqrt{(x + a)^2 + (y - 2b)^2 + (z + 2c)^2} + 2b - y}{\sqrt{(x + a)^2 + y^2 + (z + 2c)^2} - y}$$

$$F_3 = \frac{\sqrt{(x + a)^2 + (y - 2b)^2 + (-z + 2c)^2} + 2b - y}{\sqrt{(x + a)^2 + y^2 + (-z + 2c)^2} - y}$$

$$F_4 = \frac{\sqrt{(-x + a)^2 + (y - 2b)^2 + (z + 2c)^2} + 2b - y}{\sqrt{(-x + a)^2 + y^2 + (z + 2c)^2} - y}$$

$$B_y = \frac{\mu_0 M}{4\pi} \ln \left[\frac{F_5 F_6}{F_7 F_8} \right]$$

with:

$$F_5 = \frac{\sqrt{(-y + a)^2 + (x - 2b)^2 + (-z + 2c)^2} + 2b - x}{\sqrt{(-y + a)^2 + x^2 + (-z + 2c)^2} - x}$$

$$F_6 = \frac{\sqrt{(y + a)^2 + (x - 2b)^2 + (z + 2c)^2} + 2b - x}{\sqrt{(y + a)^2 + x^2 + (z + 2c)^2} - x}$$

$$F_9 = \frac{(-x + a)y}{(z + 2c)\sqrt{(-x + a)^2 + y^2 + (z + 2c)^2}}$$

$$F_{10} = \frac{(-x + a)y}{(-z + 2c)\sqrt{(-x + a)^2 + y^2 + (-z + 2c)^2}}$$

$$F_{11} = \frac{(-x + a)(-y)}{(z + 2c)\sqrt{(-x + a)^2 + y^2 + (z + 2c)^2}}$$

$$F_{12} = \frac{(-x + a)(-y)}{(-z + 2c)\sqrt{(-x + a)^2 + y^2 + (-z + 2c)^2}}$$

To simplify the calculations and simulations, we only discussed the B_z and its gradient with respect to the z , i.e., dB_z/dz , in the space inside the cube (S) in Fig. 1. In the next parts, the base of the cube (S) covers the surface of all magnets including gaps between the magnets.

3. Results and Discussion

Firstly, we have conducted simulations and calculations for B_z and dB_z/dz of a single magnet along the y axis at a distance of 10, 20, 30, 40, 50, and 100 μm from the surface of the magnet. The magnet has a surface area of $1,000 \times 1,000 \mu\text{m}^2$, a position in the Oxyz coordinates as shown in Fig. 2a. The origin is on the top surface of the magnet, i.e. all points on the top surface of the magnet have a z coordinate of 0. Simulated results are shown in Figs. 2b and 2c.

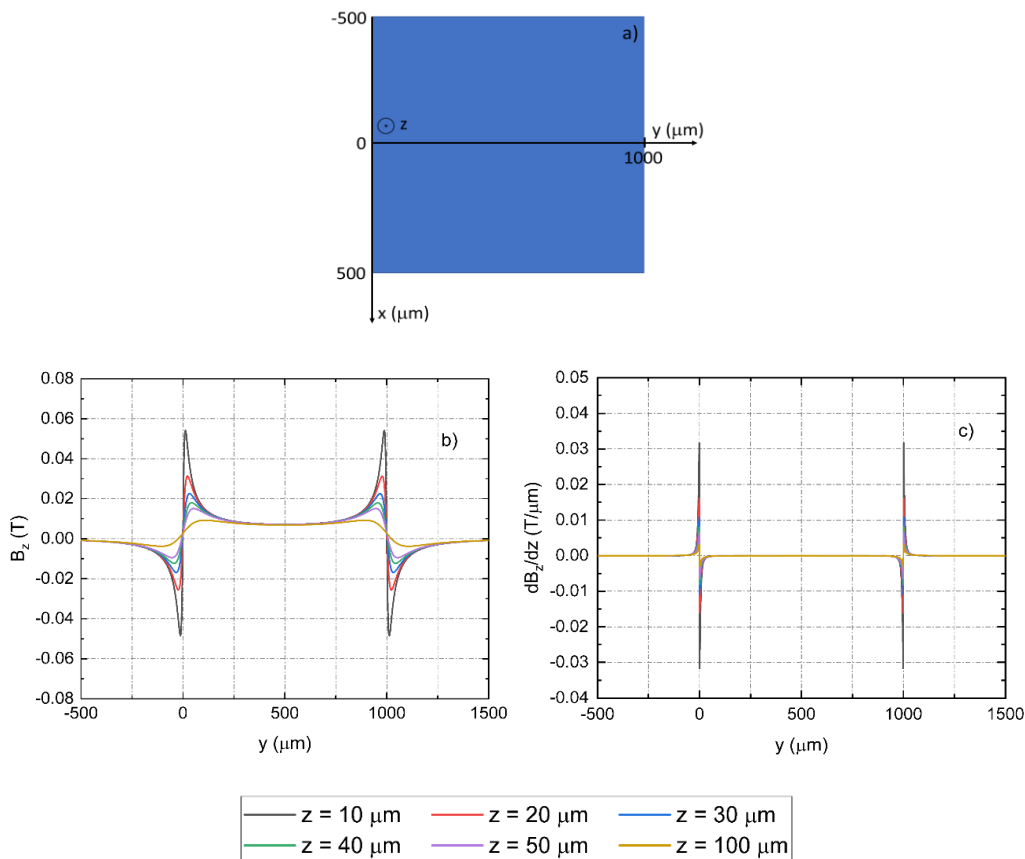


Figure 2. Simulation model for a magnet (a); simulated results for B_z (b) and dB_z/dz (c) along the y axis at a distance of 10, 20, 30, 40, 50, and 100 μm from the surface of a magnet with surface area of $1,000 \times 1,000 \mu\text{m}^2$.

It is seen clearly that the B_z and the dB_z/dz are significant only near the edges of the magnet. Both the B_z and the dB_z/dz decrease abruptly in the space (S) and far from the edges of the magnet. This means that the magnetic force component in the z axis produced by the magnet at positions far from the edges is almost zero because the magnetic force is proportional to $B_z \times (dB_z/dz)$. All are due to the distribution of the magnetic stray field of the magnet. A zero-force zone in the middle of the space (S) makes the magnet unable to separate and control micro-objects when they fall into the space (S). This is a disadvantage of the single magnets with large surface areas even if they are super hard magnets.

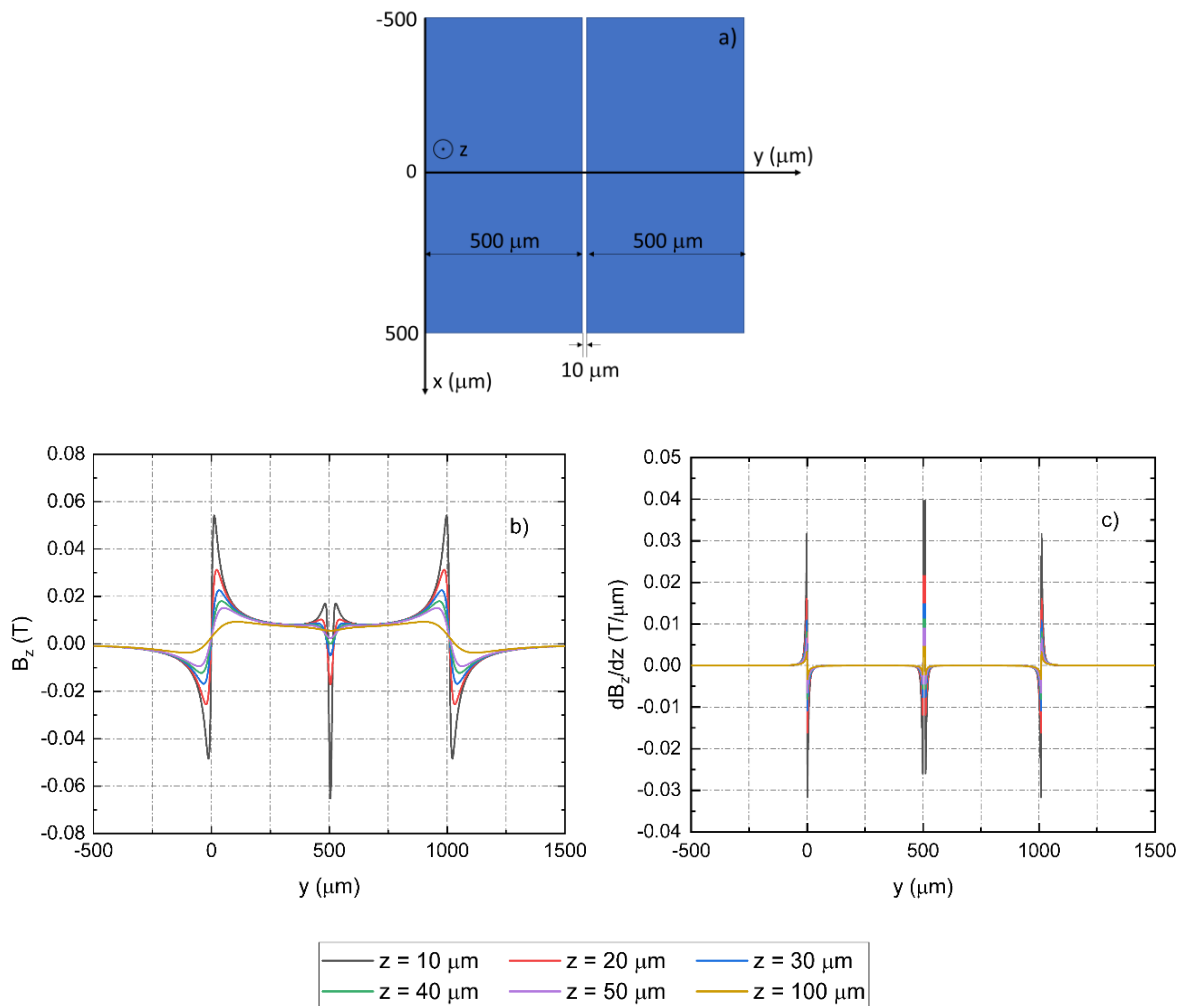


Figure 3. Simulation model for 2 magnets (a); simulated results for B_z (b) and dB_z/dz (c) along the y axis at a distance of 10, 20, 30, 40, 50, and 100 μm from the surface of an array of 2 magnets with surface area of the each one of $1000 \times 500 \mu\text{m}^2$.

Secondly, similar simulations and calculations were done for 2 smaller magnets with the surface area of the each one of $1,000 \times 500 \mu\text{m}^2$ and the distance between them of $10 \mu\text{m}$. The simulation model and results are shown in Fig. 2. One can see that, in this case, both the B_z and the dB_z/dz in the middle of the space (S), i.e., in the gap between the 2 magnets are enhanced compared to the B_z and the dB_z/dz in the middle of the space (S) in the case of the above single magnet. In terms of an absolute value, the

strength and the gradient of the magnetic field in the gap between the 2 magnets are greater than that at the borders of the space (S). The enhancement of the B_z and the dB_z/dz in the middle of the space (S) creates a large magnetic force here. Therefore, only by cutting the large magnet $1,000 \times 1,000 \mu\text{m}^2$ into the 2 smaller magnets $1,000 \times 500 \mu\text{m}^2$, we restrict partly the disadvantage of the large magnet. However, in this case, we only have one more position with the magnetic force at the space between the 2 magnets. The distance between the positions in the space (S) that have the magnetic force is still sizeable. Thus, it is also difficult to use these magnets for controlling the micro-objects.

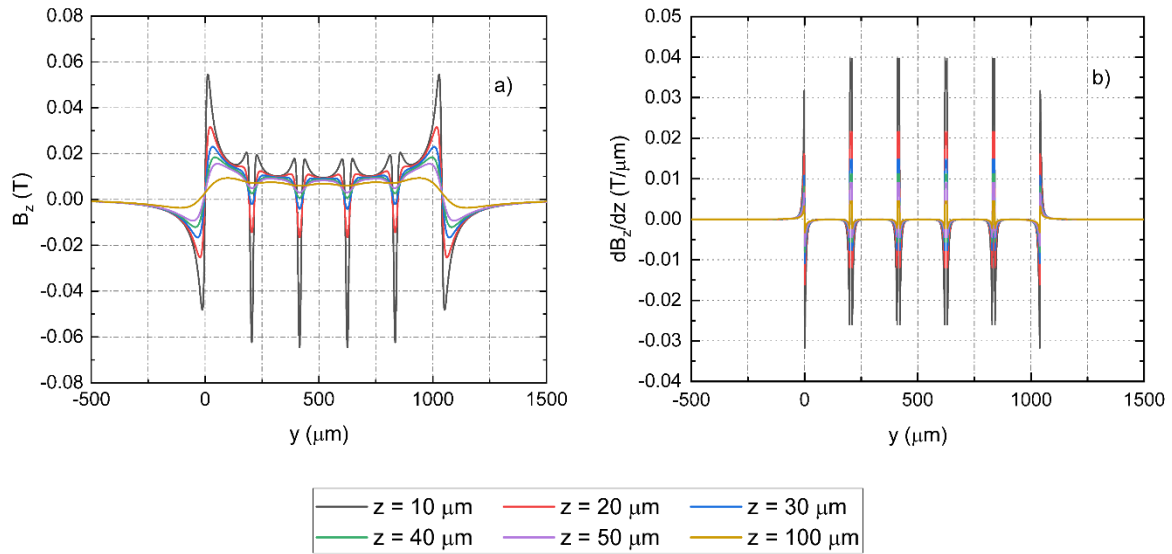


Figure 4. Simulated results for B_z (a) and dB_z/dz (b) along the y axis at a distance of 10, 20, 30, 40, 50, and 100 μm from the surface of an array of 5 magnets with surface area of the each one of $1000 \times 200 \mu\text{m}^2$.

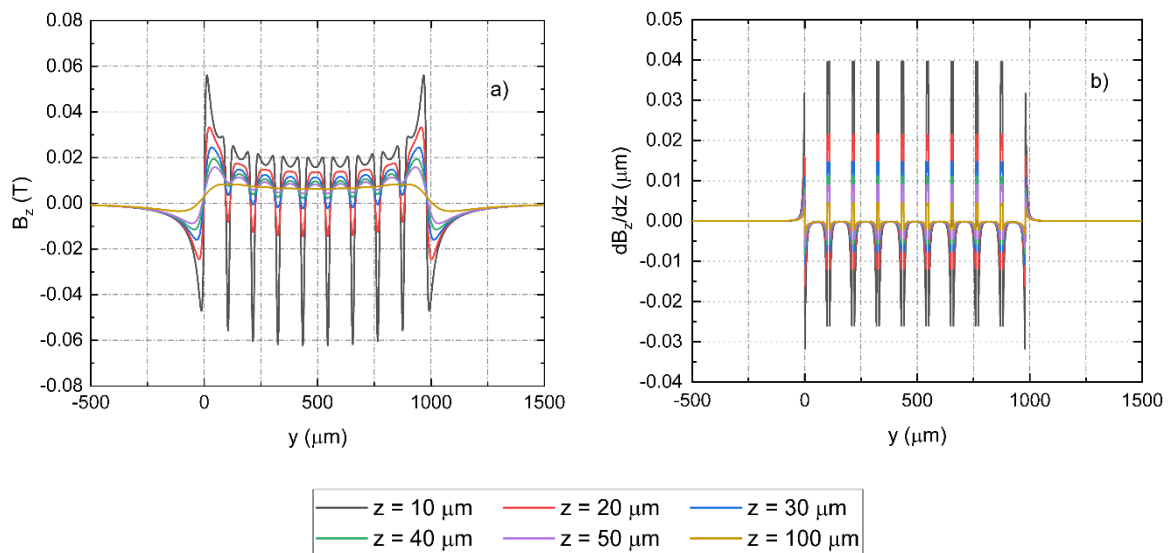


Figure 5. Simulated results for B_z (a) and dB_z/dz (b) along the y axis at a distance of 10, 20, 30, 40, 50, and 100 μm from the surface of an array of 9 magnets with surface area of the each one of $1000 \times 100 \mu\text{m}^2$.

Next, we continued to carry out comparable simulations and calculations for an array of 5 magnets with the surface area of the each one of $1,000 \times 200 \mu\text{m}^2$, an array of 9 magnets with the surface area of the each one of $1,000 \times 100 \mu\text{m}^2$, an array of 17 magnets with the surface area of the each one of $1,000 \times 50 \mu\text{m}^2$, and an array of 50 magnets with the surface area of the each one of $1,000 \times 10 \mu\text{m}^2$. The distance between the magnets in all these cases is $10 \mu\text{m}$. The B_z and the dB_z/dz of all arrays of the magnets were also simulated and calculated along the y axis at a distance of 10, 20, 30, 40, 50, and 100 μm , and are presented in Figs. 4, 5, 6, and 7.

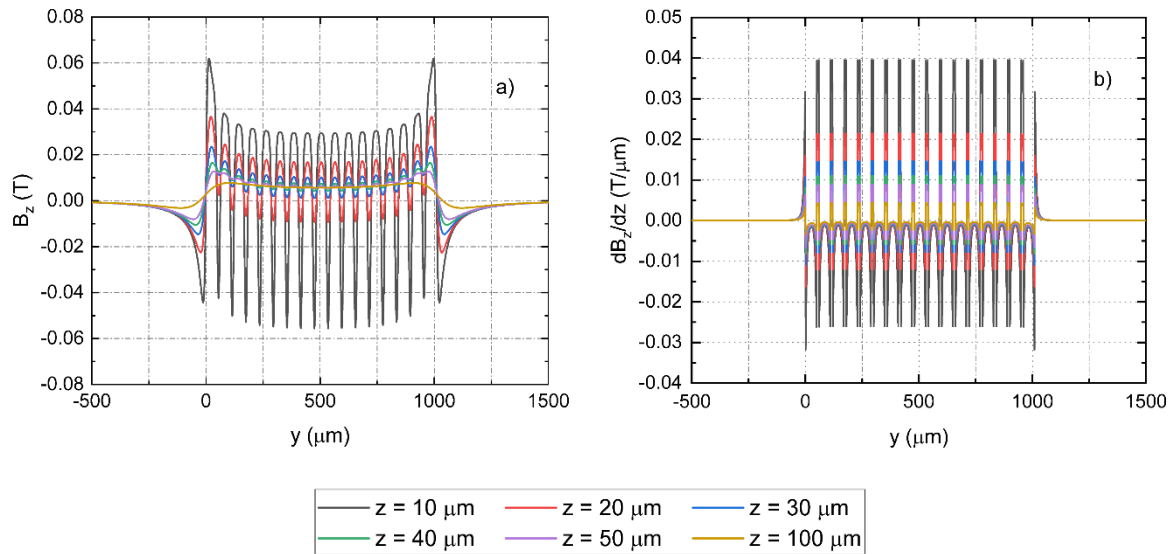


Figure 6. Simulated results for B_z (a) and dB_z/dz (b) along the y axis at a distance of 10, 20, 30, 40, 50, and 100 μm from the surface of an array of 17 magnets with surface area of the each one of $1000 \times 50 \mu\text{m}^2$.

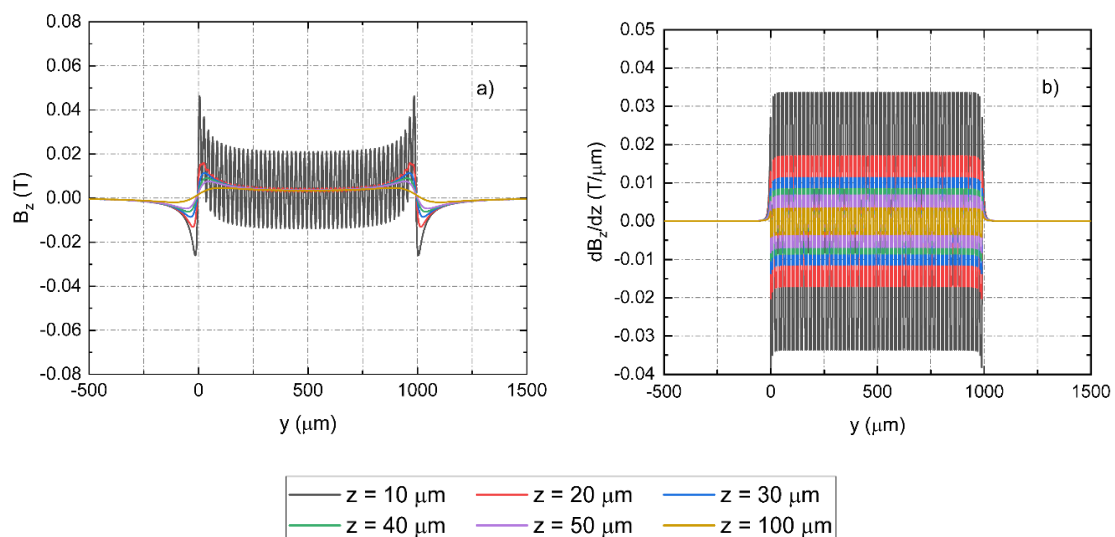


Figure 7. Simulated results for B_z (a) and dB_z/dz (b) along the y axis at a distance of 10, 20, 30, 40, 50, and 100 μm from the surface of an array of 50 magnets with surface area of the each one of $1000 \times 10 \mu\text{m}^2$.

Obtained results show that the maximum absolute values of the B_z and the dB_z/dz in the space (S) of the array of the magnets with the surface area of the each one of $1,000 \times 200 \mu\text{m}^2$, $1,000 \times 100 \mu\text{m}^2$, and $1,000 \times 50 \mu\text{m}^2$ are the same with that of the 2 magnets with the surface area of the each one of $1,000 \times 500 \mu\text{m}^2$. However, the B_z and the dB_z/dz in the space (S) become more uniform from the border to the middle when the surface area of the magnet is smaller. This means that the magnetic force produced in the space (S) by the array of the magnets with the surface area of the each one of $1,000 \times 50 \mu\text{m}^2$ is the most homogeneous compared to the force produced by the array of the larger magnets in this study. The homogeneousness can be explained by the increase in the number of magnets or by the decrease in the distance between positions that have the $|B_z|_{max}$ and the $|dB_z/dz|_{max}$. The homogeneousness and the high absolute magnitude of the B_z , the dB_z/dz , and the field of the magnetic force in the space (S) make the array of the magnets with the surface area of the each one of $1,000 \times 50 \mu\text{m}^2$ more applicable in the process of controlling and separating micro-objects comparing to the other configurations of the magnets in this work.

If we continue to down the surface area of the magnets to $1,000 \times 10 \mu\text{m}^2$, both the B_z and the dB_z/dz , consequently, the magnetic force in the space (S) produced by the array of these magnets become more homogeneous than that produced by the arrays of the larger magnets. However, in terms of magnitude, they become smaller than that produced by the arrays of the larger magnets. Obviously, we can enhance the magnitude and the homogeneousness of the magnetic field strength and gradient, as well as the field of the magnetic force in the space (S) by varying properly the surface area of the magnets.

4. Conclusion

This work has presented the obtained results of simulations and calculations for the B_z and the dB_z/dz produced by the arrays of the parallelepiped magnets having the residual magnetism of 1.6T along the z axis. Particularly, the array of a magnet with the surface area of $1,000 \times 1,000 \mu\text{m}^2$; the array of 2 magnets with the surface area of the each one of $1,000 \times 500 \mu\text{m}^2$, the array of 5 magnets with the surface area of the each one of $1,000 \times 200 \mu\text{m}^2$, the array of 9 magnets with the surface area of the each one of $1,000 \times 100 \mu\text{m}^2$, the array of 17 magnets with the surface area of the each one of $1,000 \times 50 \mu\text{m}^2$, and the array of 50 magnets with the surface area of the each one of $1,000 \times 10 \mu\text{m}^2$. The thickness of all magnets is $5 \mu\text{m}$, and the distance between the magnets is constant of $10 \mu\text{m}$. This systemic study shows that splitting a magnet with a large surface area into an array of magnets with properly smaller surface areas will enhance the magnetic field strength and gradient in the middle of the space above the magnets. Consequently, the magnetic force zone will be expanded and become more homogeneous from the outer border region of the arrays of the small magnets to the middle of the arrays instead of being only concentrated at the edges of the magnet as the case of the large magnet. The enhancement of the magnetic field strength and gradient, as well as the expansion of the magnetic force zone makes arrays of the properly small magnets more applicable in micro-objects control and separation than a large magnet.

Acknowledgments

This research was funded by VNU Asia Research Center (ARC) from grants source by CHEY Institute for Advanced Studies, code CA.22.05A.

References

- [1] K. J. Strnat, Modern Permanent Magnets for Applications in Electro-technology, Proceedings of the IEEE, Vol. 78, 1990, pp. 923-946, <https://doi.org/10.1109/5.56908>.
- [2] A. L. Gassner, M. Abonnenc, H. X. Chen, J. Morandini, J. Josserand, J. S. Rossier, J. M. Busnel, H. H. Girault, Magnetic Forces Produced by Rectangular Permanent Magnets in Static Microsystems, Lab on a Chip, Vol. 9, 2009, pp. 2356-2363, <https://doi.org/10.1039/B901865D>.
- [3] M. F. Robin, J. Marchalot, Basic Principles and Recent Advances in Magnetic Cell Separation, Magnetochemistry, Vol. 8, 2022, pp. 11-56, <https://doi.org/10.3390/magnetochemistry8010011>.
- [4] S. Rampini, P. Li, D. Gandhi, M. Mutas, Y. F. Ran, M. Carr, G. U. Lee, Design of Micromagnetic Arrays for On-chip Separation of Superparamagnetic Bead Aggregates and Detection of a Model Protein and Double-stranded DNA Analytes, Scientific Reports, Vol. 11, 2021, pp. 5302-5314, <https://doi.org/10.1038/s41598-021-84395-3>.
- [5] J. M. Camacho, V. Sosa, Alternative Method to Calculate the Magnetic Field of Permanent Magnets with Azimuthal Symmetry, Revista Mexicana de Fisica E, Vol. 59, 2013, pp. 8-17.
- [6] L. V. Cuong, N. T. Hien, P. B. Thang, P. D. Thang, Micromagnets for Bio-molecules Separation, Proceedings of the 4th International Workshop on Nanotechnology and Application, 2013, pp. 173-176.
- [7] R. Ravaut, G. Lemarquand, Magnetic Field Produced by a Parallelepipedic Magnet of Various and Uniform Polarization, Progress in Electromagnetics Research, Vol. 98, 2009, pp. 207-219, <https://doi.org/10.2528/PIER09091704>.
- [8] P. Chen, Y. Y. Huang, K. Hoshino, X. Zhang, Multiscale Immunomagnetic Enrichment of Circulating Tumor Cells: from Tubes to Microchips, Lab on a Chip, Vol. 14, 2014, pp. 446-458, <https://doi.org/10.1039/C3LC51107C>.
- [9] M. Sagawa, S. Fujimura, H. Yamamoto, Y. Matsuura, S. Hirose, Magnetic Properties of Rare-Earth-Iron-Boron Permanent Magnet Materials, Journal of Applied Physics, Vol. 57, 1985, pp. 4094-4096, <https://doi.org/10.1063/1.334629>.
- [10] J. F. Herbst, R₂Fe₁₄B Materials: Intrinsic Properties and Technological Aspects, Reviews of Modern Physics, Vol. 63, 1991, pp. 819-898, <https://doi.org/10.1103/RevModPhys.63.819>.
- [11] F. Bancel, G. Lemarquand, Three-dimensional Analytical Optimization of Permanent Magnets Alternated Structure, IEEE Transactions on Magnetics, Vol. 34, 1998, pp. 242-247, <https://doi.org/10.1109/20.650248>.
- [12] Z. J. Yang, T. H. Johansen, H. Bratsberg, G. Helgesen, A. T. Skjeltop, Potential and Force Between a Magnet and a Bulk Y₁Ba₂Cu₃O_{7-δ} Superconductor Studied by a Mechanical Pendulum, Superconductor Science and Technology, Vol. 3, 1990, pp. 591-597, <https://doi.org/10.1088/0953-2048/3/12/004>.